Dynamics of suspended sediment transport and yield in a large agricultural catchment, southwest France

Chantha Oeurng,[1] Sabine Sauvage,[1,2,*] and José-Miguel Sánchez-Pérez[1,2]

[1] Université de Toulouse, INPT, UPS, ECOLAB (Laboratoire Ecologie Fonctionnelle), Ecole Nationale Supérieure Agronomique de Toulouse (ENSAT), Castanet Tolosan, France

[2] CNRS, ECOLAB (Laboratoire Ecologie Fonctionnelle), Castanet Tolosan, France

*Correspondence to: Sabine Sauvage, Université de Toulouse,; INPT, UPS, ECOLAB (Laboratoire Ecologie Fonctionnelle), Ecole Nationale Supérieure Agronomique de Toulouse (ENSAT), Avenue de l'Agrobiopole, BP 32607 Auzeville Tolosane 31326 Castanet Tolosan Cedex, France. E-mail: sauvage@cict.fr

ABSTRACT: The dynamics of suspended sediment transport were monitored continuously in a large agricultural catchment in southwest France from January 2007 to March 2009. The objective of this paper is to analyse the temporal variability in suspended sediment transport and yield in that catchment. Analyses were also undertaken to assess the relationships between precipitation, discharge and suspended sediment transport, and to interpret sediment delivery processes using suspended sediment-discharge hysteresis patterns. During the study period, we analysed 17 flood events, with high resolution suspended sediment data derived from continuous turbidity and automatic sampling. The results revealed strong seasonal, annual and inter-annual variability in suspended sediment transport. Sediment was strongly transported during spring, when frequent flood events of high magnitude and intensity occurred. Annual sediment transport in 2007 yielded 16 614 tonnes, representing 15 t km^{-2} (85% of annual load transport during floods for 16% of annual duration), while the 2008 sediment yield was 77 960 tonnes, representing 70 t km^{-2} (95% of annual load transport during floods for 20% of annual duration). Analysis of the relationships between precipitation, discharge and suspended sediment transport showed that there were significant correlations between total precipitation, peak discharge, total water yield, flood intensity and sediment variables during the flood events, but no relationship with antecedent conditions. Flood events were classified in relation to suspended sediment concentration (SSC)–discharge hysteretic loops, complemented with temporal dynamics of SSC–discharge ranges during rising and falling flow. The hysteretic shapes obtained for all flood events reflected the distribution of probable sediment sources throughout the catchment. Regarding the sediment transport during all flood events, clockwise hysteretic loops represented 68% from river deposited sediments and nearby source areas, anticlockwise 29% from distant source areas, and simultaneity of SSC and discharge 3%.

KEYWORDS: agricultural catchment; temporal variability; sediment transport; hysteretic loops; flood events

Introduction

Suspended sediment transport has been identified as the main global mechanism of fluvial sediment transport. Walling and Webb (1986) estimated that the global amount of suspended sediment transport is about 3·5 times higher than that of solutes, while the bedload represents only a small component of fluvial transport. Suspended sediment transport from agricultural catchments to stream networks is responsible for aquatic habitat degradation, reservoir sedimentation and the transport of sediment-bound pollutants (pesticides, particulate nutrients, heavy metals and other toxic substances). Quantifying and understanding the dynamics of suspended sediment transfer from agricultural land to watercourses is essential in controlling soil erosion and in implementing appropriate mitigation practices to reduce stream suspended sediment and associated pollutant loads, and hence improve surface water quality downstream (Heathwaite *et al.*, 2005). Appropriate assessment of suspended sediment yield is of particular importance for the purpose of catchment management and therefore interest in the dynamics of suspended sediment transport has increased in recent decades (Alexandrov *et al.*, 2003a).

So far, many studies on suspended sediment transport dynamics have been conducted in small-scale agricultural catchments of less than 100 km^2 (Gao *et al.*, 2007; Lefrançois *et al.*, 2007; Estrany *et al.*, 2009; Deasy *et al.*, 2009). However, little attention has been paid to sediment dynamics in large agricultural catchments, where there are many difficulties such as spatiotemporal variability in climatic conditions, land use and soil texture. Moreover, field measurements and collection of data on suspended sediment are generally difficult tasks, rarely achieved over long timescales in large

catchments. Understanding of the catchment-scale dynamics of suspended sediment transport is limited by this lack of data and by the high spatial and temporal variability of sediment output, which in turn is associated with various factors such as precipitation characteristics, the connectivity of sediment sources varying with physical settings and human activities, changes in contributing areas and hydraulic boundary conditions (Schmidt and Morche, 2006).

Analysis of the relationships between sediment transport, precipitation and discharge characteristics can help in understanding the factors and processes determining sediment responses (Zabaleta *et al.*, 2007; Nadal-Romero *et al.*, 2008). The study of hysteretic loops in a single flood event also helps to better interpret the spatial distribution of catchment sediment sources within a drainage system (Peart and Walling, 1982; Dickinson and Bolton, 1992; Kostrenzewski *et al.*, 1994; Lefrançois *et al.*, 2007).

The Gascogne area, southwest France, located in highly contrasting zones with various climatic influences (the mountain region, the Atlantic and the Mediterranean), has been dominated by anthropogenic activities, particularly intensive agriculture, causing severe erosion in recent decades. This poses a major threat to surface water quality, since sediment transport within the catchment is the main factor in transporting contaminant sediments. Therefore, the 1110 km^2 Save catchment located in the Gascogne area was selected for this study.

The objective of this study was to analyse the temporal variability in suspended sediment transport and yield in a large agricultural catchment. Analyses were also undertaken to assess the relationships between precipitation, discharge and suspended sediment transport, and to interpret sediment delivery processes using suspended sediment-discharge hysteresis patterns.

Materials and Methods

Study area

The Save catchment, located in the area of Coteaux Gascogne, is an agricultural catchment of 1110 km^2 and has its source in the piedmont zone of the Pyrenees Mountains (southwest France) at an altitude of 600 m, joining the Garonne River after a 140 km course with a linear shape and an average slope of 3·6‰ (Figure 1).

This catchment lies on detrital sediments from the Pyrenees Mountains. It is bound on the east by the Garonne River, on the south by the Pyrenees and on the west by the Atlantic Ocean (Echanchu, 1988). Throughout the Obligocene and Miocene, this catchment served as an emergent zone of subsidence that received sandy, clay and calcareous sediments derived from the erosion of the Pyrenees Mountains, which were in an organic phase at that time. The heterogeneous materials were of low energetic value and produced a thick detrital formation of molasse type in the Miocene. From the Pleistocene onwards, the river became channelized, cutting broad valleys in the molasse deposits and leaving terraces of coarse alluvium (Revel and Guiresse, 1995). The substratum of the catchment consists of impervious Miocene molassic deposits.

In this area, which has been cultivated since the Middle Ages, mechanical erosion by ploughing has had a greater

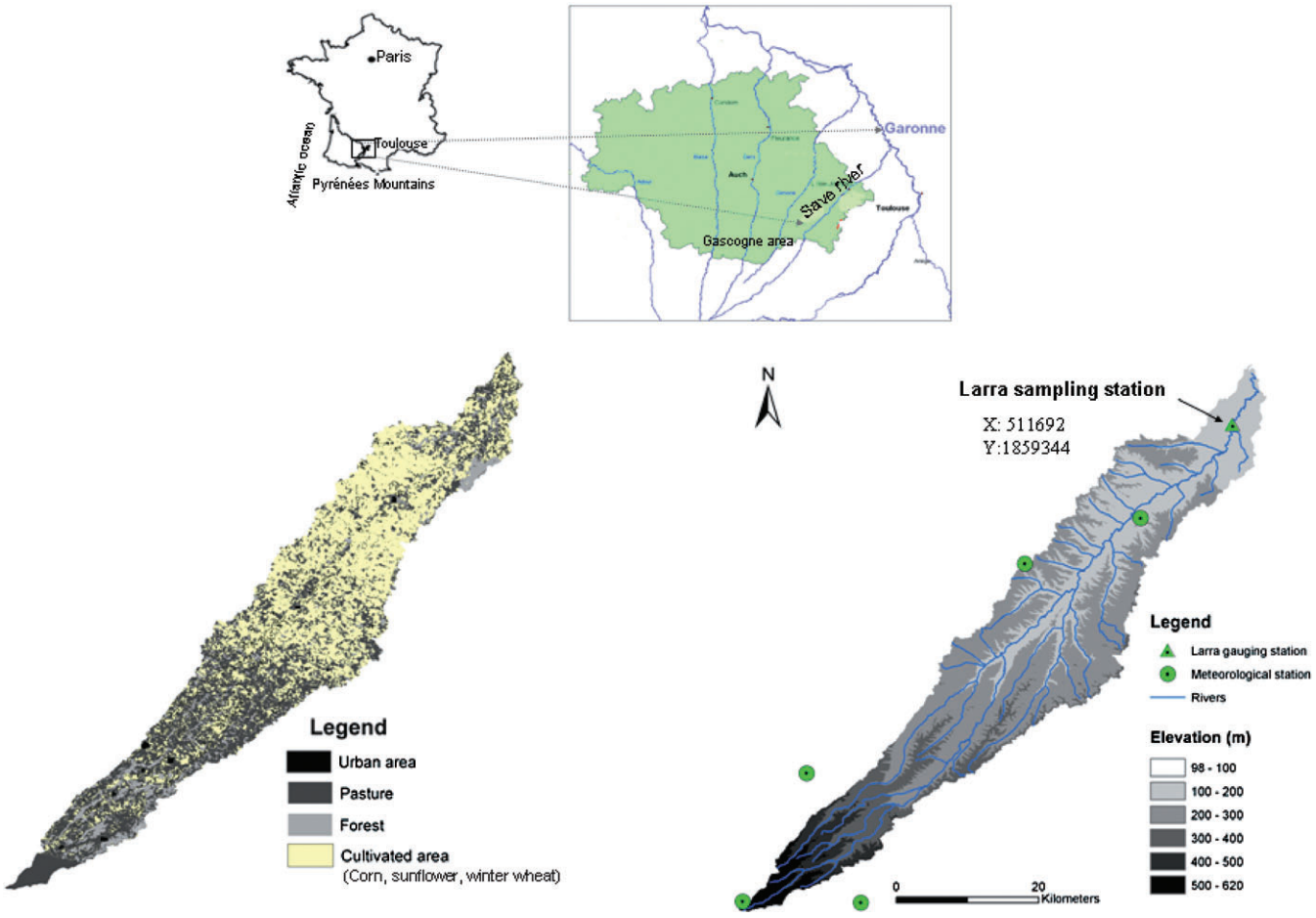

Figure 1. Location, land use and topographical maps of the Save catchment. This figure is available in colour online at wileyonlinelibrary.com/journal/espl

impact on downward soil displacement than water erosion, with a major impact on surface relief, mainly on levelling and soil distribution (Guiresse and Revel, 1995). Very weak erosion has led to the development of calcic luvisols (UN FAO soil units) on the tertiary substratum and local rendosols on the hard calcareous sandstone beds. On hillsides with very gentle slope, the calcic cambisols have been subjected to moderate erosion. Non-calcic silty soils, locally named *boulbènes*, represent less than 10% of the soil in this area. Calcic soils are dominated by a clay content ranging from 40% to 50%, while non-calcic soils are silty (50–60%). The upstream part of the catchment is a hilly agricultural area mainly covered with pastures and small amount of forest, while the lower part is flat and devoted to intensive agriculture, mostly pasture and a rotation of corn, sunflower and winter wheat (90% of the area used for agricultural purposes) (Figure 1).

The climatic conditions are oceanic, with annual precipitation of 700 to 900 mm and annual evaporation of 500 to 600 mm. The dry period runs from June to August (the month with maximum deficit) and the wet period from October to May (Ribeyeix-Claret, 2001). The hydrology regime of the catchment is mainly pluvial, i.e. regulated by rainfall (Echanchu, 1988), with maximum discharge in May and low flows during summer (July to September).

The catchment substratum is relatively impermeable due to its high clay content. Consequently, the river discharge is mainly supplied by surface and subsurface runoff, and groundwater is limited to alluvial and colluvial phreatic aquifers. The maximum discharge for the long-term period (1985–2008) is 210 $m^3 s^{-1}$ (14 June 2000), while summer discharge sustained by a nested canal at the catchment head is 0·004 $m^3 s^{-1}$ at a point 100 km downstream since water is used for irrigation along its course. The mean monthly 31-year discharge (1965–2006) is 6·29 $m^3 s^{-1}$.

Instrumentation and sampling method

A Sonde YSI 6920 (YSI Incorporated, Ohio, USA) measuring probe and Automatic Water Sampler (ecoTech Umwelt-Meßsysteme GmbH, Bonn, Germany) with 24 bottles of one litre were installed at the Save catchment outlet (Larra bridge) in January 2007. The Sonde was positioned near the bank of the river under the bridge, where homogeneity of water movement was properly considered for all hydrological conditions. The pump inlet was placed next to the Sonde pipe. The dissolved oxygen content, electrical conductivity, nitrate, pH, turbidity and water level were recorded at 10-minute intervals. The values of the different parameters in water were detected by sensors on the Sonde YSI and the data then transferred to the ecoTech memory. We programmed the Sonde to pump water when there were water level variations, Δx (in centimetres), ranging from 10 cm to 30 cm, based on seasonal hydrological conditions for both the rising and falling stage. This sampling method provided high sampling frequency during storm events. Manual sampling was also carried out using a two litre bottle lowered from the Larra bridge, near the Sonde position, at weekly intervals when water levels were not remarkably varied. During the study period, several technical problems such as sensor derivation and crushing led to occasional difficulties in measuring continuous water turbidity. We missed continuous measurements for some flood periods (15% of the total study period), but we carried out intensive manual sampling, particularly during the flood events, in order to get reliable estimates of suspended sediment load during the missing time.

Data source, treatment and analysis

Hydro-climatological data

Rainfall data from five meteorological stations in the catchment (Figure 1) were obtained from Meteo France. The mean total rainfall depth and intensity in the whole catchment were derived using the Thiessen Polygon method. Total annual rainfall during the study period in 2007 and 2008 amounted to 603 and 787 mm, respectively. Data on hourly discharge were obtained from CACG (Compagnie d'Aménagement des Coteaux de Gascogne), which is responsible for hydrological monitoring in the Gascogne region.

The discharge was plotted by the rating-curve in which water level was measured hourly by pressure at Larra gauging station in the form of a rectangular weir (length 12 m), then transferred by teletransmission. The mean total water yield of the two study years, 2007 and 2008, was 98 mm and 120 mm, respectively. These values are below the long-term mean value of 136 mm for the period 1985–2008. A year was considered dry if the annual water yield was below the long-term value. Within this context, both years can be classified as dry but the first year 2007 is very dry, since no major floods occurred in autumn. During the whole study period, between January 2007 and March 2009, there were 20 flood events and we had a reliable total of 17 recorded flood events with continuous measurement of turbidity (Figure 2). Mean discharge during the first year was 3·45 $m^3 s^{-1}$ and 4·23 $m^3 s^{-1}$

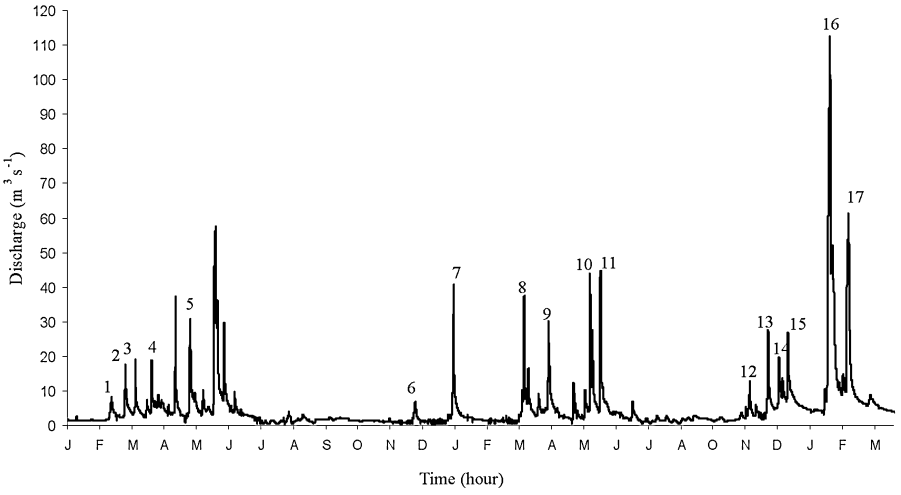

Figure 2. Hourly discharge (in $m^3 s^{-1}$) within 17 recorded flood events between January 2007 and March 2009.

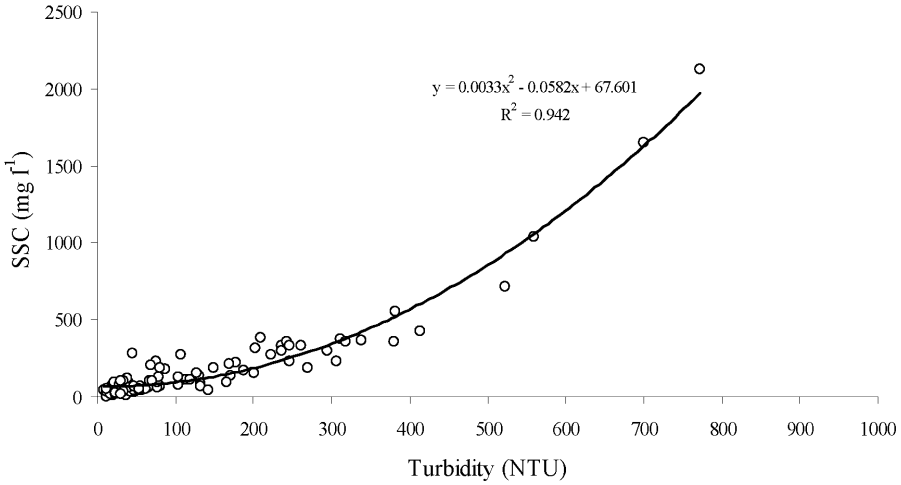

Figure 3. Relationship between recorded turbidity (in NTU) and suspended sediment concentration, SSC (in mg l^{-1}) at Larra sampling station.

during the second year. These values are below the mean annual discharge of the long-term discharge (1985–2008), which was 4·79 m^3 s^{-1}. Maximum instantaneous discharge during floods ranged from 6·75 m^3 s^{-1} (observed on 11 December 2007) to 112·60 m^3 s^{-1} (27 January 2009).

Suspended sediment concentration (SSC) and turbidity data processing

During the study period, we obtained 246 water samples through our manual and automatic sampling methods. These water samples were analysed in the laboratory to determine suspended sediment concentration (SSC) using a nitrocellulose filter (GF 0·45 µm) and drying at 40 °C for 48 hours. Volumes of water ranging from 150 to 1000 ml were filtered according particle load. SSC data determined from samples collected manually and by automatic sampling over a range of hydrological conditions and turbidity levels throughout the study period were used to generate a calibration equation between turbidity and SSC data.

The relationship between SSC and turbidity is generally a power function SSC = a(Turbidity)^n (Gippel, 1995; Lewis, 2003). However, in this case, the SSC–turbidity relationship was polynomial because of the light weight of the particles. Figure 3 illustrates the SSC–turbidity relationship for the Save catchment (best fitted with a second-order positive polynomial equation SSC = 0·0033(Turbidity)^2 – 0·0582(Turbidity) + 67·601, where SSC is measured in mg l^{-1} and turbidity in NTU (nephelometric turbidity units). Continuous SSC data were derived from this equation for the turbidity range between 0 and 800 NTU, beyond which turbidity saturation occurred. For values of turbidity higher than 800 NTU (5% of flood periods) and during missing continuous measurements of turbidity, a linear interpolation method was applied between two close sampling points to construct the continuous SSC series.

Calculation of fluxes

High frequency SSC records were derived from the relationship between SSC and turbidity. The sediment loads were calculated as the product of the hourly discharge and the corresponding SSC:

$$F = 0{\cdot}0864 \times Q_i \times \mathrm{SSC}_i$$

$$\begin{cases} \mathrm{SSC}_i = \mathrm{f(NTU)} (0 < NTU < 800) \\ \mathrm{SSC}_i = \mathrm{Interpolation}[\mathrm{SSC}_{i-1}; \mathrm{SSC}_{i+1}] \end{cases}$$

where F is daily suspended sediment flux (in tonnes per day); Q_i is the hourly water discharge (in m^3 s^{-1}), SSC_i is the corresponding suspended sediment concentration (in mg l^{-1}) and 0·0864 is the conversion factor. Accumulated suspended sediment fluxes (monthly to annual load) were calculated as the sum of fluxes during the period considered.

Statistical analyses

To assess the relationships between precipitation, discharge and sediment transport, statistical analyses were performed. A database was generated for each flood event and contained four groups of variables: antecedent conditions to the flood conditions, precipitation, discharge and suspended sediment during the flood. Variables used in the characterization of floods are summarized in Table I. Antecedent conditions are described by accumulated precipitation one day before the flood (P1d), five days before (P5d), and ten days before (P10d), by beginning baseflow (Qb) before the flood and by the antecedent flood corresponding to the flood (Qa).

Precipitation that caused the flood was characterized by mean total precipitation (Pt) and hourly maximum intensity of the precipitation (Imax). Total water yield (Wt) during the flood was expressed by the total water depth of the event, total duration of the event (Td), and mean (Qm) and maximum discharge (Qmax) corresponding to the time of rise to reach the peak discharge (Tr). The discharge speed to reach the peak flow during a flood event is defined by flood intensity, If [If = (Qmax – Qb)/Tr]. Sediment load was expressed as the mean SSC (SSCm) derived from the SSC–turbidity relationship, the maximum SSC of the event (SSCmax) and the total suspended sediment yield transported during the flood event (SST). The relationships between all these variables were investigated using statistical techniques (Pearson correlation matrix) in the STATISTICA package.

Analysis of SSC–discharge dynamics

Relationships between SSC and discharge during flood events were studied using continuous measurements. We use the term 'flood' to mean a complete hydrological event with rising and recession limbs. The typology of the SSC–discharge relationship during floods generally depends on the simultaneity or interval between the SSC peak and the discharge maximum. Typology interpretation is not unique, but varies according to

Table I. Names, abbreviations and units for the variables used to characterize flood events and to perform Pearson correlation matrix and factorial analysis

	Abbreviation	Unit
Antecedent conditions		
Accumulated precipitation 1 day before the flood	P1d	mm
Accumulated precipitation 5 days before the flood	P5d	mm
Accumulated precipitation 10 days before the flood	P10d	mm
Baseflow before the flood	Qb	$m^3 s^{-1}$
Antecedent maximum discharge	Qa	$m^3 s^{-1}$
Flood event conditions		
Flood duration	Fd	hours
Time of rise (time to reach maximum discharge)	Tr	hours
Total precipitation during the flood	Pt	mm
Maximum rainfall intensity of the flood	Imax	mm h^{-1}
Flood intensity	If	$m^3 min^{-2}$
Total water yield	Wt	mm
Mean discharge	Qm	$m^3 s^{-1}$
Maximum discharge	Qmax	$m^3 s^{-1}$
Mean suspended sediment concentration	SSCm	mg l^{-1}
Maximum suspended sediment concentration	SSCmax	mg l^{-1}
Total suspended sediment yield in tonnes	SST	tonnes

the study context. We used a typology with three classes, inspired by Williams (1989).

In the first class, peaks of SSC and discharge arrive simultaneously. The SSC–discharge plot is symmetrical between rising and falling limbs, with little or no hysteresis. In the second class, the SSC peak arrives before the discharge peak and the relationship between SSC and discharge describes a clockwise hysteretic loop. In the third class, the SSC peak arrives later than the discharge peak and the SSC–discharge relationship describes an anticlockwise hysteretic loop (Williams, 1989). Typology interpretation can also depend on other flood characteristics. We complemented this typology with an analysis of the range of SSC versus discharge during the flood. The SSC maxima depended simultaneously on stream transport capacity and discharge, and also on the availability of particles to be mobilized by the discharge (Lefrançois *et al.*, 2007). We focused on SSC maxima versus discharge to compare the variation in particle availability during the different flood events. During recession flow, a decrease in discharge leads to sediment deposition. We focused on SSC at the discharge maxima to compare the deposition capacity of the stream during the falling stage of different flood events.

Results

General description of flood events analysed

During the study period, 17 flood events were analysed (Figure 3): six events occurred in winter (January to March), five in spring (March to June) and six in autumn (October to December). The longest event (event 16; 351 hours) occurred on 27 January 2009 with total rainfall depth 74·54 mm, reaching an hourly peak discharge of 116·6 $m^3 s^{-1}$. This event is noteworthy since there was a 10-year return period and it represented a major flood event in winter 2009. During this event, sediment transport reached 23 374 tonnes. However, the event that the maximum sediment transport (event 10) took place in early June 2008, when the flood intensity was the highest of all the events observed during the study period. A total of 41 750 tonnes of sediment were transported during this extreme episode. Table II summarizes the main characteristics of flood duration, time of rise, flood intensity, precipitation, discharge and SSC associated with the floods analysed, which are described in detail later.

- The duration of the flood events varied between 105 and 351 hours, with an average value of 191 hours (Table II). Seven events were longer than average duration, while 10 events were shorter. The event on 1 June 2008 took the shortest time (16 hours) to reach the peak, while the general rising time of floods in our observed events varied from 16 hours (minimum) to 84 hours (maximum), with an average value of 41 hours. Sediment transport in early June 2008 showed the most extreme value observed during the study period (41 750 tonnes).
- The maximum discharge during flood events varied from 6·75 $m^3 s^{-1}$ to 112·60 $m^3 s^{-1}$, with an average peak value of 33 $m^3 s^{-1}$ (median = 27·57 $m^3 s^{-1}$; standard deviation (SD) = 25·05 $m^3 s^{-1}$). Rainfall amount varied from 7·46 mm to 74·54 mm (median = 20·25 mm; SD = 17·18 mm). Average rainfall intensity in the whole catchment ranged between 1·32 and 17·23 mm h^{-1} (median = 3·97 mm h^{-1}; SD = 3·72 mm h^{-1}).
- Peak SSC during flood events varied from 158 mg l^{-1}, recorded on 13 February 2007, to 15·74 g l^{-1} on 1 June 2008 (median = 691 mg l^{-1}; SD = 565 mg l^{-1}). A significant quantity of suspended sediment was transported during floods, mainly in spring season when flood magnitude was significant. The sediment load ranged from 177 to 41 750 tonnes (median = 1642 tonnes; SD = 5820 tonnes), indicating that 65% of each event transported more than 1000 tonnes.
- In terms of the typology described in the previous section, 68% of total sediment transport during all flood events demonstrated clockwise hysteresis, 29% anticlockwise and 3% simultaneity of SSC and discharge.

Temporal variability in suspended sediment transport

Within-event sediment variability

So far, due to differences between the catchments, there is only partial understanding of the internal dynamics of suspended sediment variability, even though many studies have been conducted on SSC–discharge relationships for individual

Table II. General characteristics of all flood events observed in the Save catchment during the study period (January 2007 to March 2009)[a]

Event	Flood event date	Season	Flood duration (hours)	Time of rise (hours)	Flood intensity (m^3 min^{-2})	Total rainfall (mm)	Rainfall intensity (mm h^{-1})	Baseflow before flood (m^3 s^{-1})	Mean discharge (m^3 s^{-1})	Maximum discharge (m^3 s^{-1})	Total water yield (hm^3)	Mean SSC (mg l^{-1})	Peak SSC (mg l^{-1})	Total sediment yield (tonnes)	Class[b]
1	13/02/2007	Winter	132	55	0·11	15·59	4·79	***1·89***	4·20	7·97	2·13	***73***	***158***	***177***	C
2	27/02/2007	Winter	140	30	0·47	9·59	1·37	3·61	6·67	17·62	3·82	168	468	338	S
3	09/03/2007	Winter	164	41	0·37	***7·46***	***1·32***	3·83	6·05	19·11	4·12	164	442	856	AC
4	25/03/2007	Spring	139	21	0·72	12·58	2·64	3·83	7·74	18·94	3·68	152	361	689	AC
5	02/05/2007	Spring	200	21	1·27	20·25	2·55	3·61	10·30	30·36	5·79	243	813	2200	AC
6	11/12/2007	Autumn	128	46	***0·08***	9·24	2·80	3·16	***3·46***	***6·75***	***1·71***	136	212	190	C
7	19/01/2008	Winter	184	43	0·87	19·87	3·42	3·16	10·74	40·64	7·34	652	1380	4801	C
8	28/03/2008	Spring	228	**84**	0·42	39·27	2·79	2·56	10·39	37·60	8·56	562	1160	4820	AC
9	21/04/2008	Spring	189	22	1·19	19·38	3·97	4·06	9·60	30·20	7·1	650	1536	4385	C
10	01/06/2008	Spring	228	***16***	**2·48**	49·95	**17·23**	4·28	15·70	44·02	12·75	**1597**	**15743**	**41750**	Complex
11	12/06/2008	Spring	259	29	1·40	28·47	8·46	4·28	15·01	44·80	12·61	850	1322	9077	AC
12	08/11/2008	Autumn	***105***	46	0·22	23·83	4·65	2·96	6·18	12·97	2·4	159	466	513	C
13	26/11/2008	Autumn	191	43	0·53	35·92	4·44	4·90	9·08	27·57	3·42	494	1618	2959	S
14	06/12/2008	Autumn	126	54	0·28	27·68	5·31	4·90	10·12	19·77	3·21	278	569	1018	AC
15	14/12/2008	Autumn	256	27	0·73	13·32	1·56	6·95	11·63	26·74	6·01	128	501	1085	AC
16	27/01/2009	Winter	**351**	69	1·57	**74·54**	4·13	4·06	**34·50**	**112·60**	**43·71**	337	2003	23374	C
17	11/02/2009	Winter	233	54	0·94	32·88	4·16	**9·99**	25·94	60·66	19·71	396	1030	6867	C

[a] Maximum values shown in bold typeface and minimum values shown in bold/italic typeface.

events (Mossa, 1996; Williams, 1989; Sichingabula, 1998; Rovira and Batalla, 2006). The scatter in SSC reported is attributed to the exhaustion of sediment available in the channel or to differences in sediment availability at the beginning and end of the flood (Walling and Webb, 1982; Steegen *et al.*, 2000; Steegen and Govers, 2001; Hudson, 2003). As a result, SSC and discharge during a flood often present hysteretic behaviour, related to a time lag between peak discharge and sediment transport. For clockwise hysteresis, SSC on the rising limb of a storm hydrograph is higher than that measured at equivalent flows on the falling limb (Rovira and Batalla, 2006). For instance, in event 16 (27 January 2009), the 50 m^3 s^{-1} discharge of the rising limb contained 1817 mg l^{-1}, while the 50·28 m^3 s^{-1} discharge of the falling limb discharge contained only 881 mg l^{-1}. The beginning of the discharge wave is supplied by easily available sediment in the channel and nearby source areas. As SSC reaches its maximum value before peak discharge, it is obvious that reduction in the amount of available sediment occurred on the falling limb. Moreover, an increase of portion of baseflow on the falling limb may cause dilution of SSC. In the case of anticlockwise hysteresis, the SSC for a given discharge on the falling limb is higher than for the same discharge on the rising limb (Salant *et al.*, 2008). As can be seen from flood event 4 (25 March 2007), the same discharge of 9·59 m^3 s^{-1} contained 251 mg l^{-1} for the falling limb and 71 mg l^{-1} for the rising limb. The suspended sediment transport in the Save catchment was also influenced by sediment exhaustion, as can be observed from three successive events which appear to show a progressive exhaustion of sediment supply (events 13, 14 and 15) and a decrease in sediment availability in the channel. These successive events were recorded on 26 November 2008 (Qmax = 27·57 m^3 s^{-1}; SSCmax = 1613 mg l^{-1}), 6 December 2008 (Qmax = 19·77 m^3 s^{-1}; SSCmax = 569 mg l^{-1}), and 14 December 2008 (Qmax = 26·74 m^3 s^{-1}; SSCmax = 501 mg l^{-1}).

Seasonal, annual and inter-annual variability

In terms of the temporal dynamics in suspended sediment transport, the Save catchment showed strong seasonal, annual and inter-annual variability during the study period (Figure 4). These seasonal variations can be analysed by considering seasonal climatic variations and weather forcing. Sediment yield in both years increased sharply in spring and slightly during summer and autumn. As can be seen in Figure 4, sediment transport from June to December 2007 nearly remained constant due to the absence of major flood events. The slope breaks of the sediment and discharge curve in early June 2008 showed drastically different conditions, since the sediment delivery during these extreme flood events reached 50 000 tonnes (63% of the annual sediment budget).

Suspended sediment transport in autumn 2007 (October to December) was only 2% of annual sediment load, whereas in autumn 2008 it was 13% of annual load. This was because there was only a minor flood event (Qmax = 6·75 m^3 s^{-1}) in autumn 2007, while many flood events reaching peak discharge of 27·57 m^3 s^{-1} occurred during autumn 2008. The sediment was strongly transported during spring (March to June), a period when there were many flood events with strong flood intensity and high amplitude occurring together with tillage operations in this agricultural catchment. In spring 2007, 79% of annual sediment load was transported, while spring 2008 accounted for 70% of annual sediment load. During summer, there were no major rainfall events that could cause floods and therefore sediment transport in summer 2007 and 2008 represented only 2% and 9% of the annual budget, respectively. During the study period there was significant seasonal variability, with sediment transport during autumn

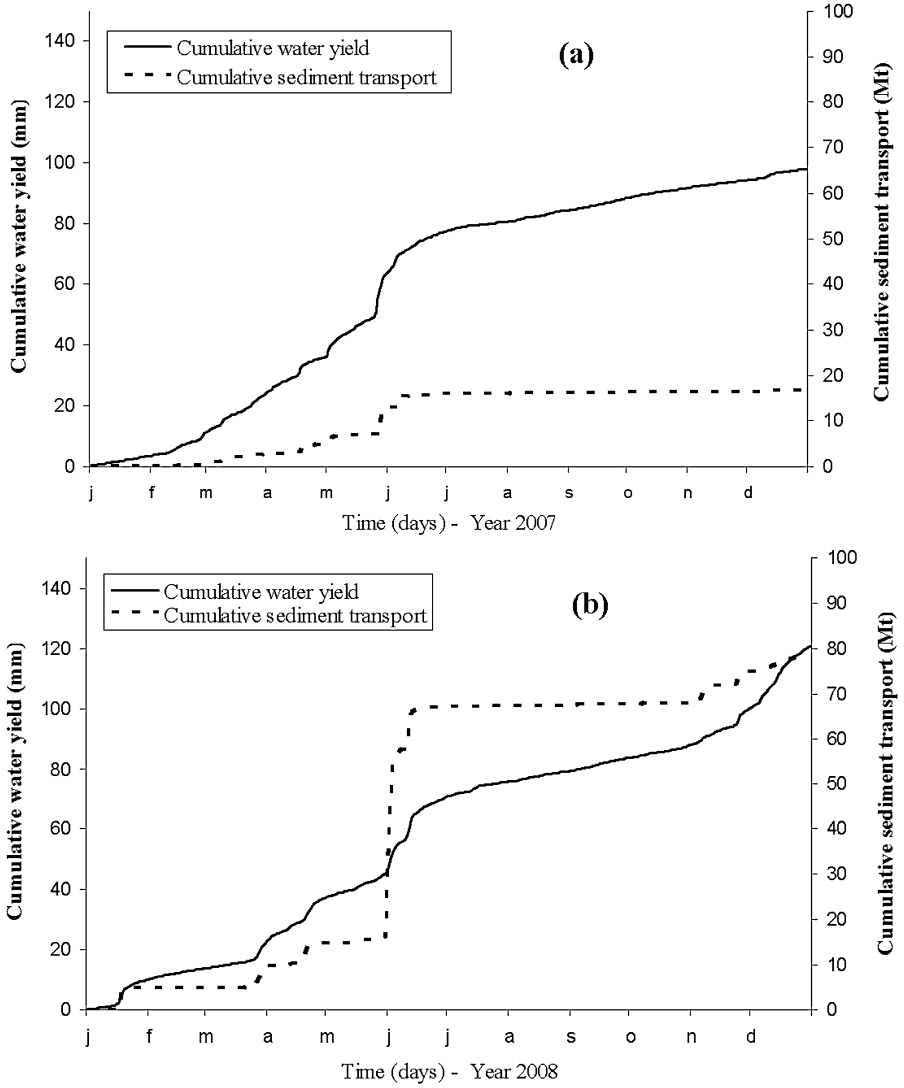

Figure 4. Cumulative water yield (in millimetres) and sediment transport (Mt) during (a) 2007 and (b) 2008.

2007 being significantly different from that in the corresponding season in 2008. Similar variations were observed in winter 2007, 2008 and 2009. Sediment transport during flood events in winter 2009 was strongly significant due to the high magnitude of two flood events (event 16 and 17), which yielded 30241 tonnes, equivalent to 182% and 39% of mean total annual load in 2007 and 2008, respectively.

The sediment transport in 2007 accounted for 16614 tonnes (85% of annual load transport during floods for 16% of annual duration) while transport in 2008 amounted to 77960 tonnes (95% of annual load transport during floods for 20% of annual duration). Although there was only a non-significant difference of 18% between total water yield in 2007 (98 mm) and 2008 (120 mm), the sediment yield in 2008 was 4·7 times higher than in 2007. In one extremely eroding event in early June 2008 (event 10), sediment transport contributed 63% of the total annual sediment budget.

Relationships between precipitation, discharge and sediment variables

In order to assess the relationships between precipitation, discharge and suspended sediment transport, which might explain the hydrological and sedimentological responses during the flood events in the Save catchment, a Pearson correlation matrix and factorial analysis that included all the above-mentioned variables (Table III) were generated for the 16 flood events. Event 10 (1 June 2008) was excluded from the matrix because it was an extraordinary event.

Table III shows the relationships between precipitation, discharge and suspended sediment transport in the Save catchment. Total precipitation (Pt) showed significant correlations with mean discharge (Qm) (R = 0·83), maximum discharge (Qmax) (R = 0·87), total water yield (Wt) (R = 0·85), maximum suspended sediment concentration (SSCmax) (R = 0·76) and suspended sediment transport (SST) (R = 0·89). The discharge variables, Qm and Qmax, were well correlated with total rainfall (Pt), but antecedent discharge (Qa) and baseflow (Qb) had only slight correlations with total precipitation (Pt).

Maximum suspended sediment (SSCmax) and suspended sediment transport (SST) showed strong relationships with total precipitation (Pt). SSCmax was well correlated with flood intensity (If) (R = 0·72) and flood duration (Fd) (R = 0·72). SST was found to be significantly correlated with total water yield (Wt) (R = 0·97) and discharge variables (Qm and Qmax). Weaker correlations were found between sediment variables and maximum rainfall intensity (Imax). Suspended sediment did not show any relationship with antecedent flow (Qa, Qb) or antecedent precipitation (P1d, P5d and P10d).

Table III. Pearson correlation matrix among all variables (n = 16)

	Fd	Tr	If	Pt	Imax	P1d	P5d	P10d	Qa	Qb	Qm	Qmax	Wt	SSCm	SSCmax	SST
Fd	1·00															
Tr	0·23	1·00														
If	**0·78**	–0·25	1·00													
Pt	**0·72**	**0·61**	0·50	1·00												
Imax	0·16	0·12	0·27	0·37	1·00											
P1d	0·04	–0·42	0·31	–0·23	–0·36	1·00										
P5d	–0·06	–0·18	0·03	–0·28	–0·28	**0·79**	1·00									
P10d	–0·12	–0·39	0·13	–0·27	0·38	0·22	0·45	1·00								
Qa	0·29	0·16	0·32	0·29	0·28	–0·39	–0·33	–0·04	1·00							
Qb	0·36	–0·09	0·28	0·13	0·02	–0·38	–0·42	–0·19	**0·69**	1·00						
Qm	**0·84**	0·34	**0·71**	**0·83**	0·25	–0·16	–0·36	–0·29	*0·53*	*0·52*	1·00					
Qmax	**0·88**	0·37	**0·75**	**0·87**	0·21	–0·05	–0·24	–0·26	0·37	0·32	**0·96**	1·00				
Wt	**0·84**	0·40	**0·68**	**0·85**	0·20	–0·07	–0·29	–0·29	0·34	0·28	**0·96**	**0·98**	1·00			
SSCm	0·43	0·05	*0·55*	0·35	*0·56*	–0·08	0·09	0·39	0·26	0·07	0·29	0·38	0·24	1·00		
SSCmax	**0·72**	0·21	**0·72**	**0·76**	0·35	–0·04	–0·05	0·00	0·21	0·15	**0·66**	**0·77**	**0·66**	**0·76**	1·00	
SST	**0·85**	0·39	**0·72**	**0·89**	0·33	–0·04	–0·23	–0·17	0·24	0·14	**0·90**	**0·97**	**0·97**	0·40	**0·77**	1·00

Note: Correlation is significant at $p < 0·01$ level for bold numbers and $p < 0·05$ for italics.

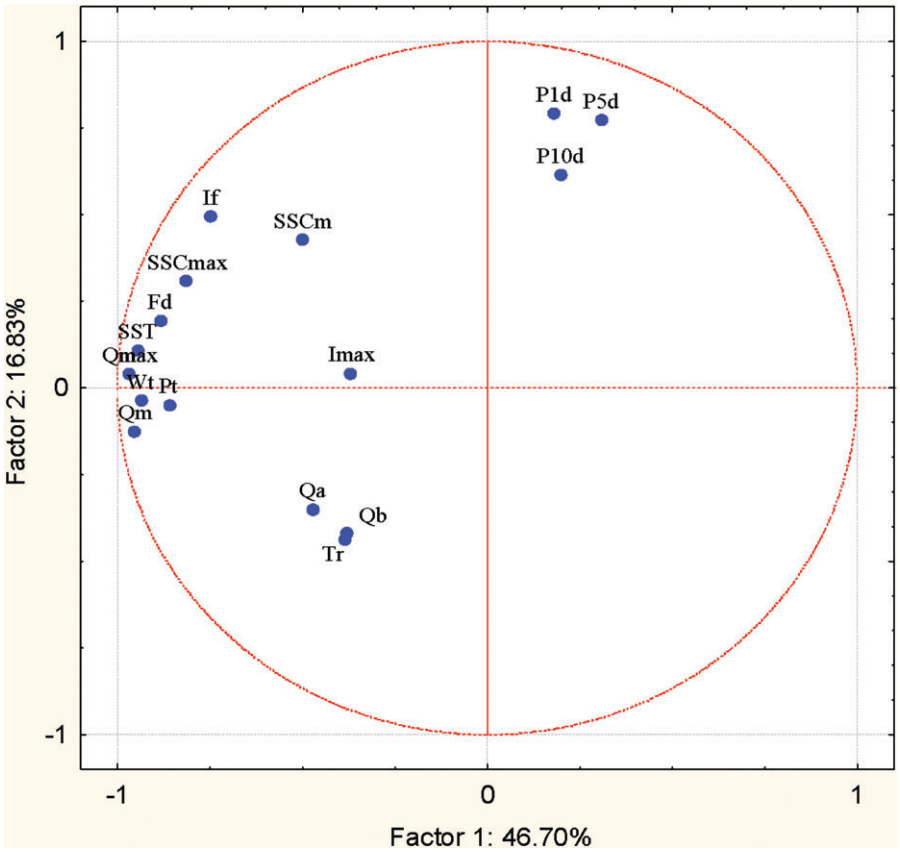

Figure 5. Location of variables included in the correlation matrixes in the factorial plane of principal component analysis. The figure is available in colour online at wileyonlinelibrary.com/journal/espl

Taking all these data into account, principal component analysis (PCA) was performed. This analysis (Figure 5) grouped in the first factor Fd, Qm, Qmax, Pt, Wt and SST, explaining 46·70% of the variance. In the second factor, If, SSCm, SSCmax and Imax were grouped, explaining 16·83% of the variance. In a 1–2 factorial plane, total sediment yield during flood events (SST) showed a strong relationship with these two factors, although the correlation was better with factor one, and no relationship was found with antecedent conditions to the flood event. The results indicate a direct response of the catchment to rainfall events in terms of discharge and suspended sediment transport during flood events.

SSC–discharge hysteresis patterns

The behaviour of suspended sediment and changes in SSC during flood events are not only a function of energy conditions, i.e. sediment is stored at low flow and transported under high flow conditions, but are also related to variations in sediment supply and sediment depletion. These changes in sediment availability result in so-called hysteresis effects (Asselman, 1999).

The relationship between discharge and SSC was analysed for all the individual flood events observed in the Save catchment. In general, we found highly variable relationships

between discharge and sediment response during different seasonal flood events (Figure 6). The different patterns of hysteresis express various probable sources of sediment spreading throughout the catchment. Seven of 17 flood events recorded during the study period showed clockwise hysteretic loops (class 2) (Figure 6b), while seven events displayed anticlockwise hysteretic loops (class 3) (Figure 6c). Two events presented class 1 behaviour (Figure 6a), indicating that SSC and discharge arrived simultaneously. However, one event (event 10, which occurred in early June 2008), showed complex mixing of clockwise and anticlockwise loops (Figure 6d) when there were multiple peaks of discharge together with multiple peaks of SSC during a flood event, coinciding with extreme rainfall intensity.

Discussion

Temporal variability of suspended sediment transport and yield

The analysis of the SSCs collected at different temporal scales (within events, seasonal and annual variability) in the Save catchment provides an insight into the characteristics of the suspended sediment load variability in a large agricultural catchment in southern Pyrenees region. Increasing SSC on the falling limb during floods may be related to sources of relatively more available sediment with lower soil aggregate stability. Such sediment sources are located at the far end of the area contributing to surface runoff, and thus sediment reaches the stream mainly during the falling limb. This may be due to soil particles, eroded within the catchment, not reaching the stream during previous rainfall-runoff events and settling on the slope, before being transported by surface runoff into the stream during the next event. The variability in event sediment transport during successive peaks of similar magnitude is influenced by sediment exhaustion effects. The Save catchment shows a pattern similar to that observed in other catchments in the Mediterranean region, e.g. in the Tordera catchment (Rovira and Batalla, 2006). An example is the progressive reduction in suspended load at different temporal scales (within floods and within multiple-peak events, during a succession of events, and seasonally) related to the exhaustion of sediment availability. Alexandrov *et al.* (2003b) observed that due to a sediment exhaustion effect, SSC levels during secondary floods in the Nahal Eshtemoa basin (Israel) were lower than those observed during a primary flood. This can be attributed to the role of in-channel sediment storage, which controls suspended sediment transport during inter-flood periods of stable flow (Smith and Dragovich, 2008). Therefore, after a period of relatively high sediment transport (supply-rich floods), sediment becomes less and less available from the channel (exhaustion phenomenon) and sediment concentrations recorded during successive floods events are consequently lower (Walling, 1978).

The total specific sediment yields in 2007 and 2008 amounted to 15 t km^{-2} and 70 t km^{-2}, respectively. This may be linked to the different characteristics of flood events, such as flood duration, rainfall intensity and flood amplitude, and other controlling factors related to soil conditions and agricultural practices in the Save catchment during both study years. The first hydrological year of the study (2007) was very dry, since there were very few rainfall events during autumn and less sediment was transported during floods with low duration and flood magnitude. Flood intensity is also a main factor to determine sediment transport. The maximum flood intensity in 2007 was only 1·27 m^3 min^{-2}, while one event in spring 2008 exhibited the maximum flood intensity of 2·48 m^3 min^{-2}, yielding a suspended sediment load of 63% of annual sediment yield in 2008. Sediment was slightly transported by baseflow during summer (2% of annual load in 2007, 9% in 2008). Although there were some rainfall events in summer during the study period, soil conditions were dry and little runoff was generated, as large amounts of rainfall infiltrated into the soil.

The annual total specific sediment yields in the Save catchment (15–70 t km^{-2}) are within the range of specific yields reported for the Garonne River, which vary from 11 to 74 t km^{-2} yr^{-1} (Coynel, 2005), but lower than the values for Mediterranean basins of the Iberian Peninsula (100–200 t km^{-2} yr^{-1}) reported by Walling and Webb (1996). Located in the same Gascogne region as the Save catchment, with the same climatic conditions, geology (molasse) and agricultural land use, the 1330 km^2 Baïs catchment and the 970 km^2 Gers catchment have specific sediment yields (63 and 41 t km^{-2} yr^{-1}, respectively) that are of a similar order of magnitude to that of the Save catchment (Maneux *et al.*, 2001). In comparison with other French catchments of similar size in the Mediterranean area, the Save values are higher than those reported for the 1100 km^2 Dronne upstream catchment (8–13 t km^{-2} yr^{-1}) but similar to those in the 1172 km^2 upstream catchment at Ariège (57–59 t km^{-2} y^{-1}) (Veyssy, 1998). The Save values are also comparable to those of the 900 km^2 Tordera catchment (50 t km^{-2} yr^{-1}) in northeast Spain (Rovira and Batalla, 2006), but much lower than the 414 t km^{-2} yr^{-1} reported for the 445 km^2 Isábena catchment (southern central Pyrenees). However, the latter catchment is highly erodible and experiences frequent floods (López-Tarazon *et al.*, 2009).

Sediment delivery process using SSC–discharge hysteresis

SSC–discharge hysteresis patterns are the outcome of the complex interaction of processes and controls that determine event discharge and catchment erosion and sediment transport. These patterns reflect the combination of sediment supply from dominant sources with the capacity of flows to transport the supplied sediment to the catchment outlets. Sediment delivery processes can be interpreted using SSC–discharge hysteresis patterns. For class 1, only two events were recorded in late winter and mid-autumn (events 2 and 13). This class is classically interpreted as the mobilization and transport of particles with unrestricted availability during the flood for the range of discharge concerned (Jansson, 2002). So far, there is little literature describing the sediment sources from this class. However, according to Hudson (2003), at low discharge sediment could come from fine deposited sediment, whereas at high discharge sediment could originate from coarser deposited sediment and/or from bank and channel hydrological erosion. When discharge is principally linked to surface runoff, sediment could originate from remote areas, particularly via surface soil erosion (Lefrançois *et al.*, 2007). Topsoil sources are therefore likely to dominate drain flow sediment in agricultural catchments (Foster *et al.*, 2003).

Clockwise hysteretic loops (class 2), which were observed in seven events in the Save catchment, generally occurred in late winter and mid-autumn, particularly in November when early seasonal rainfall started. During the periods when sediment was stored in the channel and distributed within the catchment tributaries, these sediments were transported only

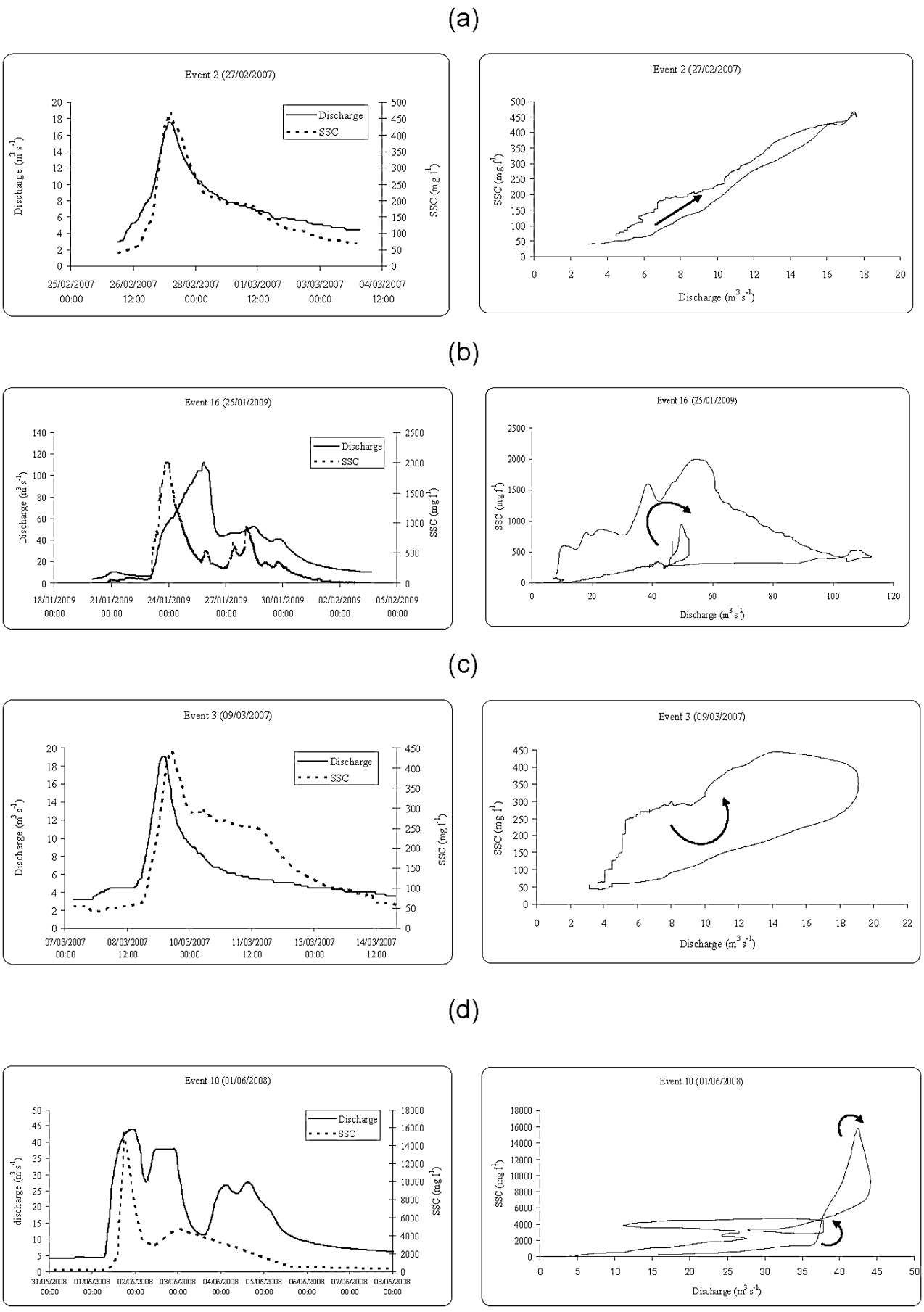

Figure 6. Examples of different types of hysteresis observed in the Save catchment during the study period (2007–2009).

after there were flood events with sufficient transport capacity. Therefore, this class could be explained by the transport of nearby available sediment and deposited sediment within the riverbed during the previous season. This can be also classically interpreted as the mobilization of particles with restricted availability during the flood event for the range of discharge concerned. Particles are believed to come from the removal of sediment deposited in the channel, with decreasing availability during the event (Lenzi and Lorenzo, 2000; Steegen *et al.*, 2000; Jansson, 2002; Goodwin *et al.*, 2003). Particle production by erosion cannot resupply the decrease in sediment stock deposits. The hypothesis of an important contribution by hillslope soils can be dismissed. Various patterns of hysteresis have been reported previously in the literature, with clockwise hysteretic loops being the most common (Walling, 1977; Klein, 1984; Williams, 1989; Jansson, 2002; Hudson, 2003; Rovira and Batalla, 2006). Klein (1984) assumed that clockwise hysteresis occurred when the sediment source area is the channel itself or an adjacent area located close to the catchment outlet, with runoff triggering the movement of sediment accumulated in the channel during the previous seasons and with little or no contribution from the tributaries. López-Tarazon *et al.* (2009) also emphasized that the clockwise phenomenon was found preferentially when rainfall was mostly located near the catchment outlet. For instance, in the Save catchment, this was the case for clockwise flood events in early autumn (events 1 and 12) and late winter (events 7, 16 and 17). For event 6, which happened on 11 December 2007 (late autumn), clockwise flood events were also found, since there was only one flood event during this season and sediment was apparently transported from deposited sediment along the channel. The role of agricultural practices in downstream areas of the Save catchment, which are mainly dominated by a crop rotation of corn, sunflower and winter wheat, was also a key determinant of sediment sources. Tillage activities here are generally carried out in April and September. Soil was eroded and then transported to the stream networks near the catchment outlet, characterized by a clockwise pattern when there were flood events reaching the capacity to bring those sediments to the outlet.

Heidel (1956) and Williams (1989) reported that for small streams, the maximum SSC usually occurs prior to peak discharge. However, other authors have suggested that clockwise hysteresis reflects a progressive decline in sediment availability during the flood event or an early-stage depletion of suspended sediment (Van Sickle and Beschta, 1983; Klein, 1984; Lenzi and Lorenzo, 2000; Sayer *et al.*, 2006). These explanations are considered to be unlikely in the Save catchment, as they imply events related to high water volume associated with the hydrological response across the entire catchment (Nadal-Romero *et al.*, 2008). In contrast, the arrival of clean water from the forested headwater area in the Save catchment could partly dilute flow to reduce SSC but not total transport.

Regarding class 3, anticlockwise hysteretic loops take place when sediment sources are widely spread throughout the catchment and sediment is not rapidly exhausted. Due to the very long thin shape of the Save catchment, sediment transport from upstream and far tributaries may take a long time to reach the catchment outlet. This type of hysteretic loop was mainly found in the Save catchment in spring and late autumn, when there were high flood magnitudes with the sufficient capacity to transport sediments from distant areas of the upstream catchment to the outlet. As the upstream part of the catchment is a hilly agricultural area mainly dominated by pastures and a small amount of forest cover (Figure 1), the source of sediment could be distant sediments, hillslope soil erosion and upstream areas (Braisington and Richards, 2000; Goodwin *et al.*, 2003; Orwin and Smart, 2004). Tillage in upland pasture areas of the Save catchment is generally performed in April, a period of strong rainfall causing the major floods in the spring season. Thus sediment yield could be strongly transported from far upstream in an anticlockwise pattern. Suspended sediment can also originate from processes with slow dynamics (slower than the discharge rise), e.g. banks may collapse when bank material is sufficiently saturated. Williams (1989) suggested that anticlockwise hysteresis results from at least one of the following causes: (i) a difference between the flood wave velocity and the mean flow velocity that carries the suspended sediment, (ii) a high soil erodibility in combination with a prolonged erosion process during the flood, and (iii) a seasonal distribution of sediment production within the drainage basin. Although there was no serious investigations of bank collapse along the Save river, bank erosion was taken into account in supplying sediment sources, particularly during major floods with high flood intensity, e.g. the event in early spring 2008 (If = 2·48 m^3 min^{-2}).

Conclusions

The dynamics of suspended sediment transport and sediment yield were analysed at different temporal scales with high resolution through two years of data collection. Analysis of the variability in SSC at different temporal scales (event, seasonal, annual and inter-annual) monitored at catchment outlet (Larra sampling station) provided insights into the characteristics of suspended sediment transport in the Save catchment in southwest France. The temporal dynamics of suspended sediment transport in the Save catchment showed strong within-event, seasonal, annual and inter-annual variability. The sediment was strongly transported during spring, when many flood events with high magnitude and intensity occurred and tillage work was performed. Sediment transport in 2007 yielded 16 614 tonnes (85% of annual load transport during floods for 16% of annual duration), while the 2008 yield was 77 960 tonnes (95% of annual load transport during floods for 20% of annual duration).

Statistical analyses revealed a significant correlation between total precipitation, peak discharge, total water yield and sediment variables during the flood events, but no relationship with antecedent conditions. These results indicate a direct response of the catchment to rainfall events, discharge and flood intensity, as well as suspended sediment transport during the flood events. The variability over different temporal scales of discharge and SSC resulted in different hysteretic patterns. Two classes (classes 2 and 3) were the most common types observed in the Save catchment. Clockwise hysteresis (class 2) mainly occurred in late winter and mid-autumn, particularly in November, while anticlockwise hysteresis (class 3) was mostly found in spring and late autumn. The hysteretic shapes obtained for all flood events reflected the distribution of probable sediment sources throughout the catchment. Of sediment transport during all flood events, clockwise hysteretic loops represented 68% from river deposited sediments and nearby sources areas, anticlockwise 29% from distant source areas, and simultaneity of SSC and discharge 3%.

With only two years of recordings, it is difficult to characterize inter-annual variability in a large agricultural catchment like the Save due to strong seasonal and annual hydrological variations. Therefore, modelling work should be conducted to characterize long-term variability in flux and to study past soil erosion following the identification of critical sediment source areas in the catchment.

Acknowledgements—This research was financially supported by a doctoral research scholarship from the French government in cooperation with Cambodia. This study was performed within the framework of the GIS-ECOBAG, Programme P2 "Garonne Moyenne" and "IMAQUES", and supported by funds from CPER and FEDER (grants n°OPI2003-768) of the Midi-Pyrenees Region and Zone Atelier Adour Garonne (ZAAG) of PEVS/CNRS347 INSUE. We sincerely thank the CACG for discharge data and Meteo France for meteorological data. The authors would like to thank Gael Durbe and ECOLAB staff for access to the site and assistance with monitoring instruments. The authors would also like to acknowledge helpful comments from Alexandra Coynel and Eric Maneux and particularly from two anonymous referees whose comments greatly improved the manuscript.

References

Alexandrov Y, Laronne JB, Reid I. 2003a. Suspended sediment concentration and its variation with water discharge in a dryland ephemeral channel, northern Negev, Israel. *Journal of Arid Environments* **53**: 73–84.

Alexandrov Y, Laronne JB, Reid I. 2003b. *Suspended Sediment Transport in Flash Floods of the Semiarid Northern Negrev, Israel*. IAHS Publication 278. IAHS Press: Wallingford; 346–352.

Asselman NEM. (1999). Suspended sediment dynamics in a large basin: the River Rhine. *Hydrological Processes* **13**: 1437–1450.

Braisington J, Richards K. 2000. Suspended sediment dynamics in small catchments in the Nepal Middle Hills. *Hydrological Processes* **14**: 2559–2574.

Coynel A. 2005. *Erosion mécanique des sols et transferts géochimiques dans le bassin Adour-Garonne*, PhD Thesis, University of Bordeaux.

Deasy C, Brazier RE, Heathwaite AL, Hodgkinson R. 2009. Pathways of runoff and sediment transfer in small agricultural catchments. *Hydrological Processes* **23**: 1349–1358.

Dickinson A, Bolton A. 1992. *A Program of Monitoring Sediment Transport in North Central Luzon, the Philippines, Erosion and Sediment Transport Monitoring Programs in River Basins*. IAHS Publication 210. IAHS Press: Wallingford; 483–492.

Echanchu D. 1988. *Géochimie des eaux du basin de la Garonne. Transfers de matières dissoutes et particulaires vers l'océan atlantique*, PhD Thesis, University of Paul Sabatier, Toulouse.

Estrany J, Garcia C, Batalla RJ. 2009. Suspended sediment transport in a small Mediterranean agricultural catchment. *Earth Surface Processes and Landforms* **34**: 929–940.

Foster IDL, Chapman AS, Hodgkinson RA, Jones AR, Lees JA, Turner SE, Scott M. 2003. Changing suspended sediment and particulate phosphorus loads and pathways in underdrained lowland agricultural catchment; Herefordshire and Worcestershire, UK. *Hydrobiologia* **494**(1–3): 119–126.

Gao P, Pasternack GB, Bali KM, Wallender WW. 2007. Suspended-sediment transport in an intensively cultivated watershed in southeastern California. *Catena* **69**: 239–252.

Gippel CJ. 1995. Potential of turbidity monitoring for measuring the transport of suspended solids in streams. *Hydrological Processes* **9**: 83–97.

Goodwin TH, Young AR, Holmes GR, Old GH, Hewitt N, Leeks GJL, Packman JC, Smith BPG. 2003. The temporal and spatial variability of sediment transport and yields within the Bradford Beck catchment, West Yorkshire. *The Science of the Total Environment* **3114–3116**: 475–494.

Guiresse M, Revel JC. 1995. Erosion due to cultivation of calcareous clay soils on hillsides in south-west France. II. Effect of ploughing down the steepest slope. *Soil Tillage* **35**(3): 157–166.

Heathwaite AL, Dils RM, Liu S, Carvalho L, Brazier RE, Pope L, Hughes M, Philips G, May L. 2005. A tiered risk-based approach for predicting diffuse and point source phosphorus losses in agricultural areas. *The Science of the Total Environment* **344**(1–3): 225–239.

Heidel SG. 1956. The progressive lag of sediment concentration with flood waves. *Transactions – American Geophysical Union* **3**(1): 56–66.

Hudson PF. 2003. Event sequence and sediment exhaustion in the lower Panuco Basin, Mexico. *Catena* **52**: 57–76.

Jansson MB. 2002. Determining sediment source areas in a tropical river basin, Costa Rica. *Catena* **47**: 63–84.

Klein M. 1984. Anti-clockwise hysteresis in suspended sediment concentration during individual storms. *Catena* **11**: 251–257.

Kostrenzewski A, Stach A, Zwolinski Z. 1994. Transport of suspended load in the Parseta River during the flash flood of June 1988, Poland. *Geographia Polonica* **63**: 63–73.

Lefrançois J, Grimaldi C, Gascuel-Odoux C, Gilliet N. 2007. Suspended sediment and discharge relationship to identify bank degradation as a main sediment source on small agricultural catchments. *Hydrological Processes* **21**: 2923–2933.

Lenzi MA, Lorenzo M. 2000. Suspended sediment load during floods in a small stream of the Dolomites (northeastern Italy). *Catena* **39**: 267–282.

Lewis J. 2003. Turbidity-controlled sampling for suspended sediment load estimation. In *Erosion and Sediment Transport Measurement in Rivers: Technological and Methodological Advances*, Bogen J, Fergus T, Walling DE (eds), Proceedings of the Oslo Workshop, June 2002, IAHS Publication 283. IAHS Press: Wallingford; 13–20.

López-Tarazon JA, Batalla RJ, Vericat D, Francke T. (2009). Suspended sediment in a highly erodible catchment: The River Isábena (southern Pyrenees). *Geomorphology* **109**: 210–221.

Maneux E, Probst JL, Veyssy E, Etcheber H. 2001. Assessment of dam trapping efficiency from water residence time: Application to fluvial sediment transport in the Adour, Dordogne, and Garonne River basins (France). *Water Resources Research* **37**: 801–811.

Mossa J. 1996. Sediment dynamics of the lowermost Mississippi River. *Engineering Geology* **45**: 457–479.

Nadal-Romero E, Latron J, Marti-Bono C, Regüés D. 2008. Temporal distribution of suspended sediment transport in a humid Mediterranean badland area: The Araguás catchment, Central Pyrenees. *Geomorphology* **97**: 601–616.

Orwin JF, Smart CC. 2004. The evidence for paraglacial sedimentation and its temporal scale in the deglacierizing basin of Small River Glacier, Canada. *Geomorphology* **58**: 175–202.

Peart MR, Walling DE. 1982. Particle size characteristics of fluvial suspended sediment. In *Recent Developments in the Explanation and Prediction of Erosion and Sediment Yield*. IAHS Publication 137. IAHS Press: Wallingford; 397–407.

Revel JC, Guiresse M. 1995. Erosion due to cultivation of calcareous clay soils on the hillsides of south west France. I. Effect of former farming practices. *Soil Tillage Research* **35**(3): 147–155.

Ribeyeix-Claret C. 2001. *Agriculture et Environnement en Gascogne Gersoise. Erosion du sol et pollution diffuse par phosphore. Le cas du basin versant d' Audradé (Gers)*, PhD Thesis, University of Toulouse.

Rovira A, Batalla R. 2006. Temporal distribution of suspended sediment transport in a Mediterranean basin: The Lower Tordera (NE Spain). *Geomorphology* **79**: 58–71.

Salant N, Hassan M, Alonso C. 2008. Suspended sediment dynamics at high and low storm flows in two small watersheds. *Hydrological Processes* **22**: 1573–1587.

Sayer AM, Walsh RPP, Bidin K. 2006. Pipeflow suspended sediment dynamics and their contribution to stream sediment budgets in small rainforest catchment, Sabah, Malaysia. *Forest Ecology and Management* **224**: 119–130.

Schmidt KH, Morche D. 2006. Sediment output and effective discharge in two small high mountain catchments in the Bavarian Alps, Germany. *Geomorphology* **80**: 131–145.

Sichingabula HM. 1998. Factors controlling variations in suspended sediment concentration for single-valued sediment rating curves, Fraser River, British Columbia, Canada. *Hydrological Processes* **12**: 1869–1894.

Smith HG, Drogovich D. 2008. Sediment budget analysis of slop-channel coupling and in-channel sediment storage in an upland catchment, south-eastern Australia. *Geomorphology* **101**: 643–654.

Steegen A, Govers G, Nachtergaele J, Takken I, Beuselink L, Poesen J. 2000. Sediment export by water from an agricultural catchment in the Loam Belt in central Belgium. *Geomorphology* **33**: 25–36.

Steegen A, Govers G. 2001. Correction factors for estimating suspended sediment export from loess catchments. *Earth Surface Processes and Landforms* **26**: 441–449.

Van Sickle J, Beschta RL. 1983. Supply-based models of suspended sediment transport in streams. *Water Resources Research* **19**(3): 768–778.

Veyssy E. 1998. *Transfers des matières organiques des basins versants aux estuaries*, PhD Thesis, University of Bordeaux.

Walling DE. 1977. Assessing the accuracy of suspended sediment rating curves for a small basin. *Water Resources Research* **13**: 531–538.

Walling DE. 1978. Suspend sediment and solute response characteristics of River Exe, Devon, England. In *Research in Fluvial Systems*, Davidson-Arnott R, Nickling W (eds). Geoabstracts: Norwich; 167–197.

Walling DE, Webb BW. 1982. Sediment availability and the prediction of storm-period sediment yields. In *Recent Development in the Explanation and Prediction of Erosion and Sediment Yield*. IAHS Publication 137. IAHS Press: Wallingford; 327–337.

Walling DE, Webb BW. 1986. Solutes in river systems. In *Solute Process*, Trudgill ST (ed.). John Wiley & Sons: Chichester; 251–320.

Walling DA, Webb BW. 1996. *Erosion and Sediment Yield: A Global Overview*. IAHS Publication 236. IAHS Press: Wallingford; 3–19.

Williams GP. 1989. Sediment concentration versus water discharge during single hydrologic events in rivers. *Journal of Hydrology* **111**: 89–106.

Zabaleta A, Martínez M, Uriarte JA, Antigüedad U. 2007. Factors controlling suspended sediment yield during runoff events in small headwater catchments of the Basque Country. *Catena* **71**: 179–190.